

Effect of Oxygen Content in Silicon Suboxide Nanoparticles on UV Radiation Shielding

Jaewoo Lee, Sangyoon Lee, Jun Heo, and Sung Oh Cho*

Dept. of Nuclear and Quantum Engineering, Korea Advanced Institute of Science and Technology (KAIST),
291, Daehak-ro, Yuseong-gu Daejeon, Republic of Korea, 34141

*Corresponding author: socho@kaist.ac.kr

1. Introduction

UV rays as well as ionizing radiation are known to be harmful to human health, particularly skin surface. The UV spectrum consists of three ranges depending on its wavelength; UVA (315-400 nm), UVB (280-315 nm), and UVC (100-280 nm). The UVC rays are mostly blocked by the ozone layer, while the UVA and UVB reach the ground surface. Therefore, the key to UV radiation protection is to block UVA and UVB.

Meanwhile, nonstoichiometric silicon suboxide (SiO_x , $0 < x < 2$) is a promising oxide material due to its high chemical stability and good mechanical properties [1]. In particular, it is widely applied to semiconductors and optical coatings thanks to the outstanding optical properties of SiO_x . Moreover, these inherent properties can be maximized if SiO_x forms nanostructures. For this reason, SiO_x nanoparticles can be a good candidate for UV shielding.

However, a different oxidation state means a distinguishable chemical state. As a result, the material properties may vary depending on the x -values, which are related to the oxidation number of silicon. Different levels of oxidation may result in changes in UV absorption or wavelength range. Here, we show the UV shielding characteristic of SiO_x nanoparticles and propose the optical role according to oxygen content.

2. Experimental Section

2.1 Materials

P-type silicon wafer (<100>, boron-doped, 0.001-0.003 Ω cm) was procured from Tasco, USA. The wafer was cut into 1.0 mm \times 0.5 mm rods using arc discharge in the water. Reagent-grade ammonium fluoride (NH_4F) was purchased from Sigma-Aldrich, USA. The electrolyte was prepared with deionized (DI) water.

2.2 Sample Preparation

Diverse metal oxide nanoparticles can be easily synthesized by anodization [2]. The various oxidation state of the SiO_x nanoparticles was achieved with controlled anodization parameters; applied voltage, operation temperature, electrode distance, and so on. Prior to anodization, the Si rod was cleaned by sonicating in acetone and ethanol each for 5 min followed by rinsing with DI water and drying with an air stream. Anodization was performed in a two-electrode

system with a Si rod as an anode and a Pt sheet (10 mm \times 40 mm \times 0.5 mm) as a cathode as depicted in Fig. 1. Anodization of Si rod was conducted in 10 M NH_4F aqueous solution. Constant voltage (7.5, 10, and 12.5 V) was applied using a DC power supply and all anodization time was kept at 1 hr. The operation temperature was set constant at 5°C to prevent considerable heat generation due to the high resistance of Si. During anodization, the Si rod was converted into light brown precipitate and this precipitate was firstly filtered with a vacuum filtering system after anodization. The filtered precipitate was washed with DI water several times to remove any type of impurities. Then, the obtained wet powder was dried and kept in a desiccator at room temperature.

2.3 Sample Characterization

The produced powder was characterized using field emission scanning electron microscope (FESEM, Magellan400, FEI, USA) and X-ray photoelectron spectroscopy (XPS, K-alpha, Thermo VG Scientific, USA) analysis. The particle size of powder was directly measured from the FESEM images with the diameters of at least 100 particles. XPS analyzed the chemical state of particles with Al $K\alpha$ radiation (1486.7 eV). The UV shielding property was evaluated using an ultraviolet-visible spectrophotometer (UV-Vis, Lambda 1050, Perkin Elmer, USA). UV-Vis analysis was conducted by measuring the absorbance of UV rays according to wavelength.

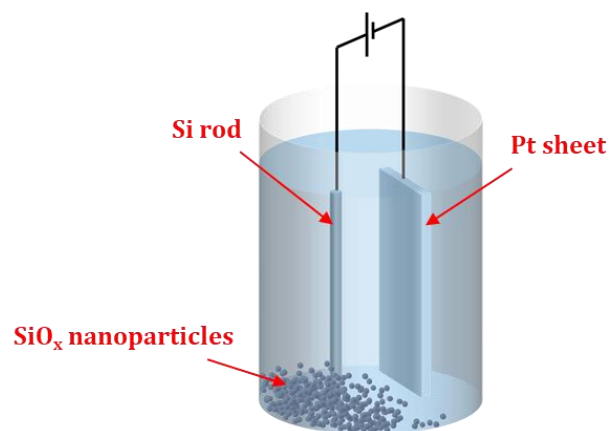


Fig. 1. Schematic view of anodization system.

3. Results and Discussion

3.1 Synthesis of Silicon Suboxide Nanoparticles

Three SiO_x powder samples were obtained through anodization at each anodization voltage. Fig. 2 shows the shape and size of the SiO_x nanoparticles fabricated. The average size of nanoparticles is found to be ~62.9 nm when 7.5 V is applied. As the applied voltage increases, the size of nanoparticles tends to increase very slightly (~66.3 nm for 10 V and ~73.6 nm for 12.5 V).

The elemental distribution of electrochemically synthesized SiO_x nanoparticles was also investigated through the XPS survey. Significant Si peaks and O peaks are identified, and C peaks may be caused by membrane filter ingredients (Fig. 3). A sharp peak near ~150 eV is due to a plasmon. No clear peaks of electrolyte components (N or F) are observed. As a result, we have confirmed silicon oxide nanoparticles are created.

Meanwhile, the oxidation number of Si in silicon oxide can be changed depending on the anodization conditions. There are generally five oxidation numbers of Si atom (0, +1, +2, +3, and +4), each combined with a different number of O atoms to form a tetragonal structure. Above five structures have different binding energies and are randomly combined each other to form an amorphous phase of SiO_x. These tetragonal structures

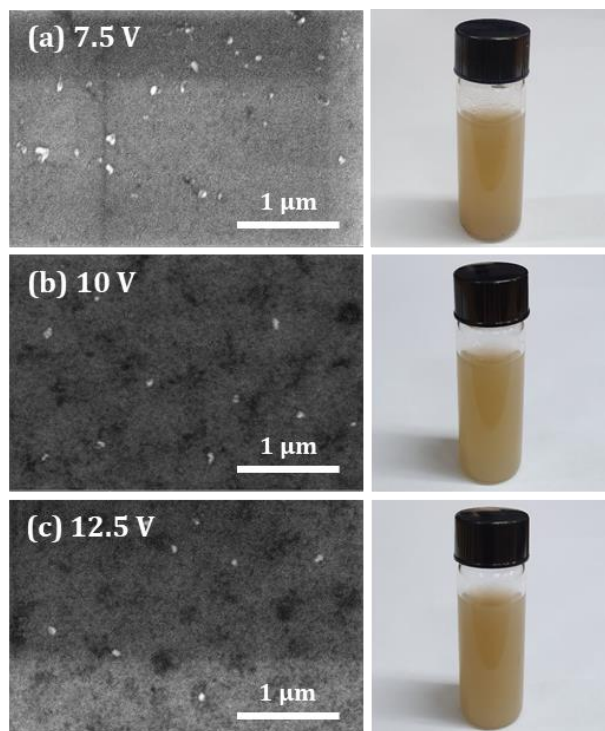


Fig. 2. FESEM images and digital photographs of SiO_x nanoparticles synthesized at each anodization voltage; (a) 7.5, (b) 10, and (c) 12.5 V.

corresponding to each oxidation number and the chemical structures formed within any SiO_x are shown in Table 1. The first Si represents the central atom, and the parentheses represent the atoms at each vertex of the tetrahedron. The binding energy of Si-(Si₄) is two due to spin-orbit splitting [3]. With the help of five structures, the x-values of SiO_x can be determined as expressed in Eq. 1.

$$x = \frac{0.0 \times a + 0.5 \times b + 1.0 \times c + 1.5 \times d + 2.0 \times e}{a + b + c + d + e} \quad (1)$$

where, *a*, *b*, *c*, *d*, and *e* are the XPS peak area of each oxidation number (0 to 4).

The Si 2p spectra of each sample are given in Fig. 4. The x-value of SiO_x shows an increasing trend as the applied voltage increases. It suggests more O²⁻ ions react with Si compared with OH⁻ ions which are produced during anodization. Consequently, SiO_x nanoparticles with different oxidation numbers (SiO_{0.55}, SiO_{0.64}, and SiO_{1.01}) were obtained.

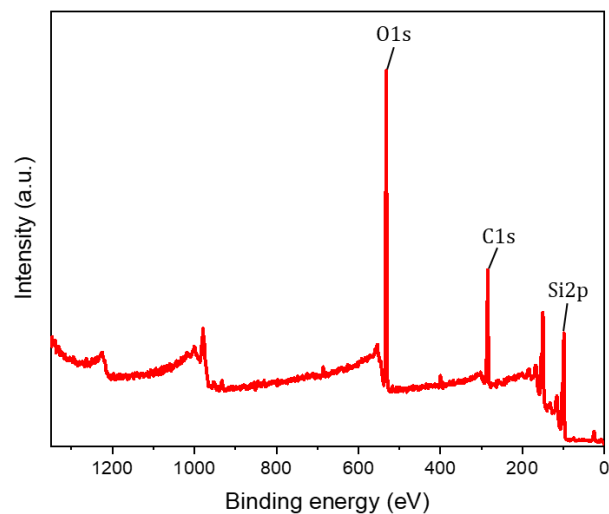


Fig. 3. XPS element survey of SiO_x nanoparticles synthesized at 7.5 V.

Table 1. The oxidation number of Si and binding state with O

Oxidation number	Tetragonal structure	Chemical structure	Binding energy (eV)
0	Si-(Si ₄)	Si	98.9/99.5
1	Si-(Si ₃ O)	Si ₂ O	100.0
2	Si-(Si ₂ O ₂)	SiO	101.0
3	Si-(SiO ₃)	Si ₂ O ₃	102.0
4	Si-(O ₄)	SiO ₂	103.1

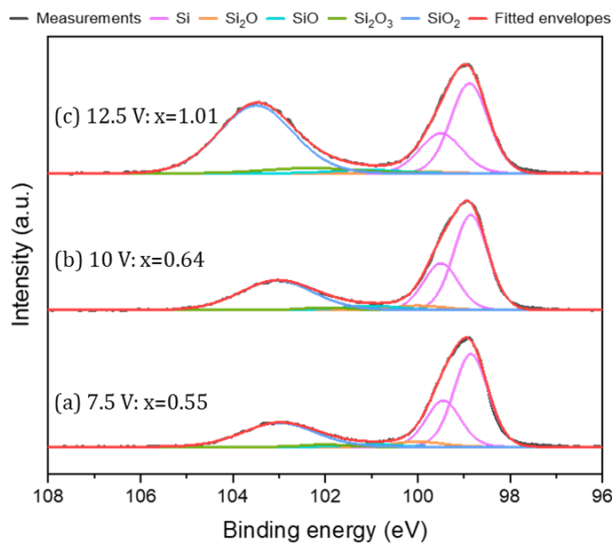


Fig. 4. XPS Si 2p spectra of SiO_x nanoparticles synthesized at each anodization voltage and calculated x -values after peak deconvolution; (a) 7.5, (b) 10, and (c) 12.5 V.

3.2 UV Absorption Analysis

The synthesized SiO_x nanoparticles were exposed to photons with various wavelengths. The absorption capacity of photons, generally, is defined by absorbance. The absorbance is calculated as Eq. 2.

$$\text{Absorbance} = \log \frac{I_0}{I} \quad (2)$$

where, I_0 is the initial intensity of photons before absorption and I is the final intensity of photons after absorption. Fig. 5 shows the absorbance of SiO_x nanoparticles produced at each anodization voltage. In the UV region, the absorbance appears in the range of 0.7 to 0.9 depending on the wavelength, particularly about 0.85 in the UVA and UVB regions. This result shows the intensity of photons transmitted through the SiO_x nanoparticles is about 14.1% of the initial intensity, so it can be seen 85.9% of UVA and UVB are absorbed. The absorbance is slightly higher as the oxygen content of the SiO_x nanoparticles decreases. This is because the number of oxygen vacancies increases as the x value decreases, resulting in a reduction in the band gap. It is known a lower optical band gap causes greater UV absorption. The photon absorption is attributed to the excitation of electrons in the valence band into the conduction band and can be interpreted as Tauc plot [4]. Interestingly, significant absorption of visible light (400-700 nm) also occurs, and the absorbance is markedly reduced from near-infrared rays (~ 700 nm). Consequently, SiO_x nanoparticles with lower oxygen content exhibit better UVA and UVB absorption. Nevertheless, since other material properties of SiO_x nanoparticles also change according to oxygen content, it is necessary to synthesize optimal SiO_x nanoparticles considering other factors.

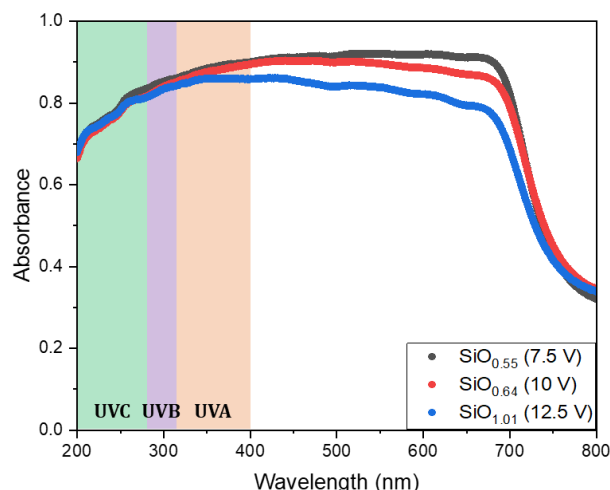


Fig. 5. Photon absorbance of $\text{SiO}_{0.55}$, $\text{SiO}_{0.64}$, and $\text{SiO}_{1.01}$ nanoparticles.

4. Conclusions

This study investigated the optical property of SiO_x nanoparticles with respect to UV ray absorption. Various SiO_x nanoparticles with different x -values were synthesized via an electrochemical method, anodization. The particles had a size of ~ 70 nm and showed a slight increase in the size when a higher voltage was applied. The oxygen content (i.e., x -value) of synthesized SiO_x nanoparticles was determined by Si 2p peak scan. As a result, $\text{SiO}_{0.55}$, $\text{SiO}_{0.64}$, and $\text{SiO}_{1.01}$ nanoparticles were obtained according to the anodization voltage.

Meanwhile, photons of various wavelengths, including UV rays, were irradiated in each SiO_x nanoparticles. Absorption of about 85.9% occurred for UVA and UVB in three SiO_x nanoparticles, and absorption increased as oxygen content decreased. A possible explanation is that oxygen vacancies increase as oxygen content decreases, leading to a reduction in optical band gaps. However, the theoretical study of the material properties of SiO_x nanoparticles is still not fully understood, so it is worth further investigation.

REFERENCES

- [1] N. Tomozeiu, Silicon Oxide (SiO_x , $0 < x < 2$): a Challenging Material for Optoelectronics, Optoelectronics – Materials and Techniques, Prof. P. Predeep (Ed.), ISBN: 978-953-307-276-0, InTech, 2011.
- [2] G. Ali, Y. J. Park, J. W. Kim, and S. O. Cho, A Green, General, and Ultrafast Route for the Synthesis of Diverse Metal Oxide Nanoparticles with Controllable Sizes and Enhanced Catalytic Activity, ACS Appl. Nano Mater., Vol.1, pp.6112-6122, 2018.
- [3] J. F. Moulder, W. F. Stickle, P. E. Sobol, and K. D. Bomben, Handbook of X-ray Photoelectron Spectroscopy, Perkin-Elmer Corp., 1992.
- [4] Q. Abbas, Understanding the UV-Vis Spectroscopy for Nanoparticles, J. Nanomater. Mol. Nanotechnol., Vol.8(3), 2019.